



**HAL**  
open science

# Numerical Estimation of the Electric Force Induced by a Cylinder-to-Cylinder EHD Device

Ihssan Matar, Christophe Louste, Michel Daaboul

► **To cite this version:**

Ihssan Matar, Christophe Louste, Michel Daaboul. Numerical Estimation of the Electric Force Induced by a Cylinder-to-Cylinder EHD Device. 2023 IEEE 22nd International Conference on Dielectric Liquids (ICDL), Jun 2023, Worcester, France. pp.1-4, 10.1109/ICDL59152.2023.10209166 . hal-04428705

**HAL Id: hal-04428705**

**<https://univ-poitiers.hal.science/hal-04428705>**

Submitted on 31 Jan 2024

**HAL** is a multi-disciplinary open access archive for the deposit and dissemination of scientific research documents, whether they are published or not. The documents may come from teaching and research institutions in France or abroad, or from public or private research centers.

L'archive ouverte pluridisciplinaire **HAL**, est destinée au dépôt et à la diffusion de documents scientifiques de niveau recherche, publiés ou non, émanant des établissements d'enseignement et de recherche français ou étrangers, des laboratoires publics ou privés.

# Numerical Estimation of the Electric Force Induced by a Cylinder-to-Cylinder EHD Device

Ihssan Matar  
EHD Team, PPRIME Institute  
University of Poitiers  
Poitiers, France  
ihssan.matar@univ-poitiers.fr  
ORCID: 0000-0003-4775-6668

Christophe LOUSTE  
EHD Team, PPRIME Institute  
University of Poitiers  
Poitiers, France  
christophe.louste@univ-poitiers.fr  
ORCID: 0000-0002-1808-6565

Michel Daaboul  
Mechanical Engineering Department  
University of Balamand  
Al-Kurah, Lebanon  
michel.daaboul@balamand.edu.lb  
ORCID: 0000-0002-4338-7618

**Abstract**— Electrohydrodynamic (EHD) devices are considered a reliable mechanism in flow control applications. The Particle Image Velocimetry (PIV) technique can be suited to obtain the velocity fields of a flow generated by an EHD device. In this work, the estimation of the electric force generated by a symmetrical cylinder-to-cylinder EHD device is done by applying the momentum integration method on a simulated model. This method requires the presence of a velocity field as well as a pressure distribution. The pressure is calculated through its gradient while using the velocity field distribution. In this study, the force is estimated using two different integration methods of the momentum equation: on the surface and in the volume. Each type of integration is applied while using the pressure provided by the simulation results and the one calculated. The calculations are performed on a control volume surrounding the system that generates the flow. The results shown prove the legitimacy of the technique used to estimate the pressure using the velocity field as well as estimating the global force created by the EHD system. Moreover, the influence of size and location of the control volume on the force calculation is analyzed. Finally, the future of this study remains to apply this method on PIV results to estimate the electric force generated during experimental setups of the same geometry and with a similar flow pattern to the one created by the simulated model.

**Keywords**— Electrohydrodynamics, Hydrofluoroether, Direct Navier-Stokes, momentum integration method.

## I. INTRODUCTION

The operation of industrial systems operating with liquids can be enhanced by employing control devices. Electrohydrodynamic (EHD) mechanisms can present an efficient solution to control a liquid flow. In reality, EHD devices possess various advantages such as: good reliability, shortened time response when compared to other devices, and low power consumption.

Three main EHD phenomena could be applied in order to put a liquid into motion. The first, which will be applicable in this study, is the conduction phenomenon [1]; it develops at relatively low electric fields. It is based on the dissociation-recombination occurrence and also due to the creation of heterocharge layers in the locality of the electrodes. The second phenomenon is injection of ions in a dielectric liquid [2], which is obtained when the electric field reaches a threshold value. The third one is induction [3], which can happen when a thermal gradient is present.

There are three types of electric forces that can be applied on a liquid in the presence of an electric field:

- Coulomb force: proportional to electric charge of a particle.
- Dielectrophoretic force: proportional to the gradient of permittivity of a particle.
- Electrostriction force: related to the polarity of a particle and the change of its shape.

In this study, the focus is to estimate the electric force generated in this system by using the momentum integration method, over the volume and the surface, on the velocity field obtained from simulated model having the same geometry as an experimental procedure that is regarded as the focal point in the future of this work. It is then, necessary to calculate the pressure gradient using the velocity field vectors. Then, a comparison is shown between resultant forces based on pressure provided by the simulation and the one calculated for both integrations: volume and surface. Having a good agreement between the results can approve the effectiveness and efficiency of the model and the method used for calculations.

This method is established on a backward calculation from the velocity field acquired by PIV or numerical simulation. In this article, the global electric force is determined inside a fixed control volume by using the momentum equation in the integral form. This method was applied successfully in many different studies with different geometries such as: a typical blade-plane actuator [4], a dielectric barrier injection system (DBI) [5]. Also, it was successfully utilized to calculate both drag and lift coefficients from forces exerted on a wing inside a control volume [6].

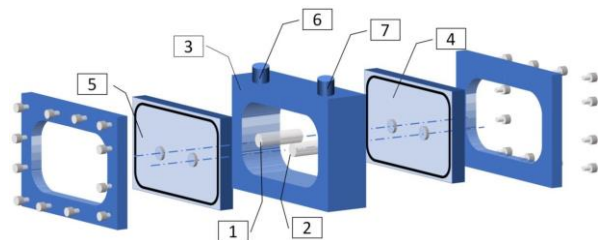


Fig. 1. Exploded view of the experimental cell

The use of the Particle Image Velocimetry (PIV) technique on electrohydrodynamic flows has allowed obtaining global velocity maps in the system. As for the simulation model it provides in addition to the velocity field vectors, a pressure distribution that will be the vital in this study to prove the legitimacy of the method used.

## II. NUMERICAL SETUP

### A. Geometrical Model

The apparatus presented in Fig. 1 consists of a 10 cm × 8 cm × 5 cm closed cell made of PMMA, filled with Hydrofluoroether Engineered Fluid (HFE-7100).

The setup is based on a symmetrical cylinder-to-cylinder electrode assembly, made of copper, installed and mounted horizontally in the middle of the tank. Both electrodes have a diameter of 2.2 cm, sat along the 5 cm depth of the cell and both being spaced by 1 cm of gap between them. A DC voltage (+ or -) is applied to either one of the electrodes while the other electrode is grounded. When a high voltage is applied to one of the electrodes, an electric force is generated which leads to the creation of a flow inside the tank.

The dielectric liquid used in these experiments is HFE7100 whose properties are given in Table I

TABLE I. PROPERTIES OF HFE 7100 AT 25°C [7]

Property		Unit
Density	1510	kg/m <sup>3</sup>
Kinematic viscosity	3.8	cSt
Electrical conductivity	1.15.10 <sup>-9</sup>	S/m
Absolute viscosity	0.58	cP
Relative permittivity	7.4	

Fig. 2 displays a PIV result of the setup and it represents the velocity contour and velocity field map of the fluid around the EHD system at work when a voltage of 2kV is applied to the cylinder on the right.

### B. Numerical Model

The theoretical model used in the simulation part was inspired from a model developed by Atten and Seyed-Yagoobi [8] and Jeong et al. [9], that was adopted by Yazdani and Seyed-Yagoobi [10]. In this study, the geometry can be considered somehow complex with no contribution of charge injection from the electrodes surface. As for the dielectric liquid; it is considered to be incompressible. In addition to that, positive and negative charge mobilities are different and in this study one specific mobility ratio of  $b_r = 10$  is considered.

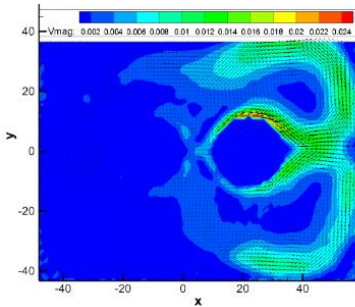


Fig. 2. Velocity contour with velocity field map at 2 KV (PIV)

The chosen geometry for the simulation, as shown in Fig. 3, is technically half the actual apparatus of the experimental part that will be studied in the future. This is chosen under the assumption that the results should be symmetrical with respect to the x-axis and for this size, reaching convergence is faster when simulating especially while having a relatively small mesh (to contain the charged layer). The mesh is created with 181201 points in 2D (half model). Fig. 3 presents also the boundary conditions applied to the model.

The system is then governed by the continuity, momentum, and Poisson's equations:

$$\nabla \cdot \mathbf{u} = 0 \quad (1)$$

$$\frac{D\mathbf{u}}{Dt} = -\frac{1}{\rho} \nabla P + \nu \nabla^2 \mathbf{u} + (n_p - n_n) \mathbf{E} \quad (2)$$

$$\nabla \cdot \mathbf{E} = \frac{(p-n)}{\epsilon}; \quad \mathbf{E} = -\nabla \phi \quad (3)$$

When it comes to normalizing the dimensions, the gap space between the two cylinders was considered as a reference value  $d = 10 \text{ mm}$ . This resulted in the creation of the following dimensionless coefficients:

$$Re_{ehd} = \frac{b_+ V}{\nu}, \quad M = \sqrt{\frac{\epsilon}{\rho b_+^2 (1 + \frac{1}{b_r})}} \quad (4)$$

$$C_0 = \frac{\sigma d^2}{b_+ \epsilon V}, \quad \alpha = \frac{D}{b_+ V} = \frac{K_B T}{eV}, \quad b_r = \frac{b_+}{b_-}$$

With the implementation of dimensionless coefficient, Equations (1), (2) and (3) become:

$$\nabla \mathbf{u} = 0 \quad (5)$$

$$\frac{d\mathbf{u}}{dt} + (\mathbf{u} \cdot \nabla) \mathbf{u} = -\left(\frac{1}{Re_{ehd}}\right) \nabla P + \frac{1}{Re_{ehd}} \nabla^2 \mathbf{u} + M^2 C_0 (p - n) \mathbf{E}$$

$$\nabla \cdot \mathbf{E} = \frac{1}{1 + (\frac{1}{b_r})} C_0 (p - n), \quad \mathbf{E} = -\nabla \phi \quad (7)$$

Fig. 5 represents the velocity glyph attained through the simulation and it shows a similar flow patten to the one in Fig.2.

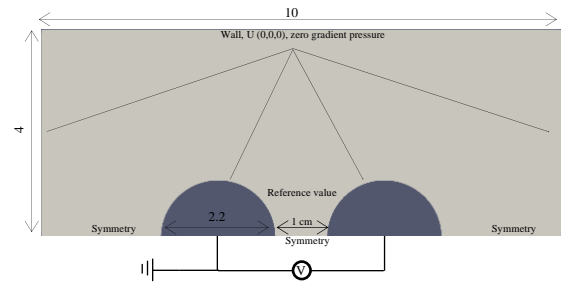


Fig. 3. Numerical geometry of the system

### C. Selection of control volume

In this study, the electric forces are produced on the circumference of the cylinders. In order to have the full spectrum of the forces present in the closed cell, it is desired to avoid interference with the edges of the closed cell and the cylinders. What is different in this case when compared to previous studies is that the obstacles, which are the cylinders, should be present inside the control volume to apply the calculation method (as seen in Fig. 4).

As mentioned earlier, one part of this work is to study the effect of the size of control volume when using the momentum equation method to calculate the force, 17 different sizes of control volume are analyzed, before touching the cylinders. These control volumes (CV) are numbered from 0 to 16, with number 0 having the largest surface without touching the edges of the tank and number 16 having the smallest surface without touching the cylinders.

### D. Force calculation

The momentum integration method is a calculation technique that enables the estimation of the electric (Coulomb) force generated by the EHD device when it is applied to the velocity field created by/present around that device. This process has been successful in various previous studies; Yan measured the mean force produced by plane-plane actuator and [4], in another study, the force produced by a DBI in a blade-blade setup [5].

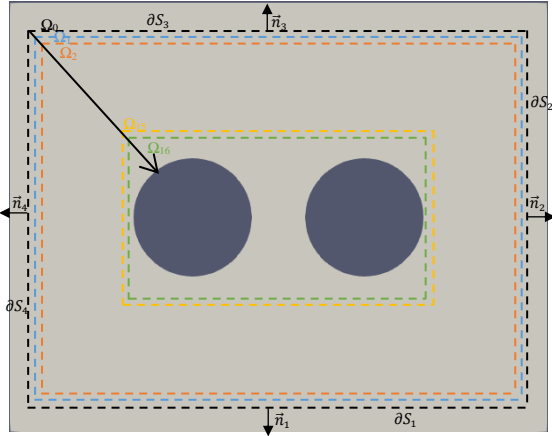


Fig. 4. Control Volume selections

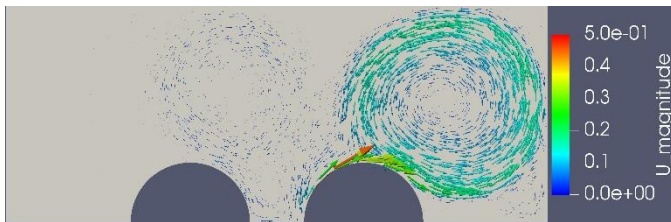


Fig. 5. Velocity glyph of the simulated model

In addition to that, this type of calculation was used by David et al. [6] to estimate the drag and lift forces exerted on a wing that led to the determination of both drag and lift coefficient.

In this paper, the force present inside the tank  $F$ , which is the resultant of electric and friction forces, is calculated by integrating the Navier-Stokes' momentum equation over a control volume  $\Omega$ .

$$\mathbf{F}(t) = \iiint_{\Omega} \frac{\partial \mathbf{u}}{\partial t} + (\rho(\mathbf{u} \cdot \nabla)\mathbf{u} + \nabla P - \rho\nu\nabla^2\mathbf{u}) d\Omega \quad (8)$$

$$\frac{\partial \mathbf{u}}{\partial t} + (\mathbf{u} \cdot \nabla)\mathbf{u} - \nu\nabla^2\mathbf{u} = -\frac{1}{\rho}\nabla P + \mathbf{F} \quad (9)$$

This study carries a different route as it focuses on one case while changing the parameters of the control volume that is

investigated to determine how the size and shape of the control volume affect the clarity of results.

In order to present that, the calculations should be devised into each term that consist the Navier-Stokes' equation and by doing so, one can determine which term is the most dominant when it comes to calculating the electric force.

First, the pressure at every point on the surface of the control volume is evaluated by integrating the pressure gradient. The computation starts at an arbitrary point  $A$  that is assigned an arbitrary pressure  $P_0$ . In this study, the arbitrary pressure is chosen to be the same as the one extracted from simulated model results at the same point to have the same starting point and be able to compare both results effectively.

$$P_M = P_0 + \int_L \nabla P(l) dl \quad (10)$$

$$\nabla P|_M = \rho \left( -\frac{\partial \mathbf{u}}{\partial t}|_M - (\mathbf{u} \cdot \nabla)\mathbf{u}|_M + \nu\nabla^2\mathbf{u}|_M \right) + \mathbf{f} \quad (11)$$

Where  $L$  is the curvilinear coordinate.

The term  $\mathbf{f}$  is neglected in the pressure gradient calculation due to the fact that the edges of the selected control volume do not touch the electrodes nor the edges of the tank.

The pressure component can be estimated for both horizontal, at  $\partial S_1$  and  $\partial S_3$ , and vertical, at  $\partial S_2$  and  $\partial S_4$ , edges.

The different terms of Naviers-Stokes' momentum equation in surface integral are as follows:

$$\text{Convective term: } \mathbf{F}_{conv} = \rho \oint_s (\mathbf{u} \cdot \mathbf{n}) \mathbf{u} \cdot d\mathbf{S} \quad (12)$$

$$\text{Pressure term: } \mathbf{F}_P = \oint_s P \cdot \mathbf{n} \cdot d\mathbf{S} \quad (13)$$

$$\text{Viscous term: } \mathbf{F}_{visc} = \oint_s \nabla \mathbf{u} \cdot \mathbf{n} \cdot d\mathbf{S} \quad (14)$$

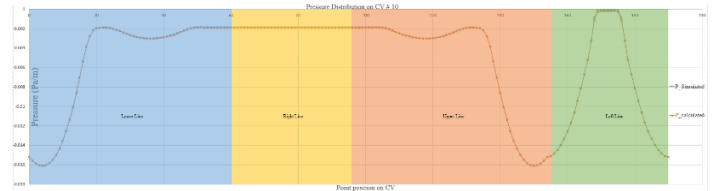


Fig. 6. Pressure distribution on the Control Volume edges for CV number 10

The total force is:

$$\mathbf{F} = \mathbf{F}_{conv} + \mathbf{F}_P - \mathbf{F}_{visc} + \text{Temporal term}$$

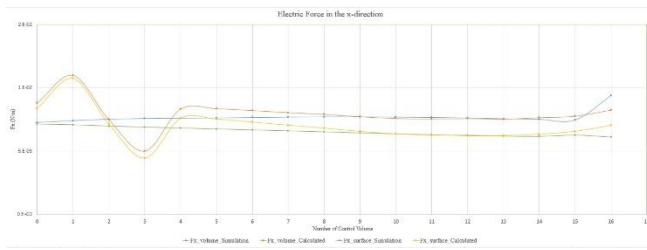


Fig. 7. Resultant Force in the x-direction in function of the control volume number

### III. DISCUSSION

The estimation of the pressure present in the system is done by calculating the pressure gradient using the velocity fields extracted from the simulation model. Fig. 6 shows both the pressure calculated and extracted from simulation results at the level of the control volume number 10, also it is divided by each edge with a starting point being at the left lower corner. The resultant graph shows a good agreement between both pressures which shows the legitimacy of the method used.

The integration of the momentum equation when applied to estimate the electric force induced by a cylinder-to-cylinder EHD system yields the results shown in Fig. 7. The graphic shows that when using the pressure extracted directly from the simulation, the resultant force is constant throughout the process of changing the size of the control volume. It is apparent that when integrating over a volume and a surface there is a difference in the outcome. Nonetheless, the difference between the results remains quasi-constant which is logical due to loss of one dimension when implementing the extracted variables.

When it comes to the results calculated through the calculated pressure, it is shown that in this case, the effect of the control volume size is more significant. This can be related to the fact that cumulative error is present when analyzing the pressure using the velocity fields. The larger the control volume is, the longer the path it would take to evaluate the pressure on the contour of the selected volume which leads to attaining more errors along the way. A fluctuation in the results appears throughout the first 5 control volume sizes. However, starting with the control volume number 5 and closing in on the system, the results start to converge towards the ones acquired through the extracted pressure until they are superimposed at control volume number 9 and remain constant until CV number 15. The resultant forces start to change at the CV number 15 although the CV does not cross the system. This can be attributed to the fact that the CV is crossing the charged layer which means it has crossed the placement of the force as well as the fact that the calculation method is based on using the variables around the CV that can interfere with the geometry of the system.

### IV. CONCLUSION

The momentum equation method was applied to a simulated model that is based geometrically on a PIV experiment. The results show good agreement when integrating the momentum equation on the volume and the surface of a selected control volume. The difference between both results remains constant which is logical due to the fact of losing a dimension during the calculations. In addition to that, the effect of the size and position of the control volume is presented and it shows that with decreasing the size of the control volume the cumulative errors decrease and it would lead to more accurate results. When the control volume is spaced out, it is shown that the calculations can lose some accuracy, but with closing in on the system in study, the resultant force becomes constant until it reaches the vicinity of the cylinders. Finally, this method will be applied to PIV results in the future that show similar flow pattern as presented by the simulated case studied in this work. This will help in estimating the force generated by the system as well as in finding an approximated ionic mobility ratio of HFE-7100 fluid when operating in EHD devices.

### REFERENCES

- [1] C. Louste, H. Romat, P. Traoré, M. Daaboul, P. Vázquez and R. Sosa, "Electroconvective Cavity Flow Patterns Created by Asymmetric Electrode Configuration," IEEE Transactions on Industry Applications, vol. 54, no. 5, pp. 4851-4856, Sept.-Oct. (2018).
- [2] S. Zhihao, D. Sun, J. Hu, P. Traoré, H.-L. Yi, and J. Wu, "Experimental study on electrohydrodynamic flows of a dielectric liquid in a needle-plate configuration under direct/alternating current electric field," Journal of Electrostatics, 106, 103454, 20
- [3] S.A. Vasilkov, V.A. Chirkov, and Yu K. Stishkov, "Study on high-voltage conductivity provided solely by field-enhanced dissociation in liquid dielectrics," Journal of Electrostatics, Volume 88, Pages 81-87, ISSN 0304-3886, (2017).
- [4] Z. Yan, Ch. Louste, Ph. Traore, H. Romat, "Experimental estimation of the electric force induced by a blade-plane actuator in dielectric liquids Journal of Electrostatics 71 (2013) pp 478-483
- [5] C. Louste, Z. Yan, Ph. Traore and M. Daaboul, "Experimental estimation of electric force induced by dielectric barrier injection", 2014 IEEE International Conference on Liquid Dielectrics, Bled, Slovenia, June-July, (2014).
- [6] David, L., Jardin, T., & Farcy, A. On the non-intrusive evaluation of fluid forces with the momentum equation approach\*. Measurement Science and Technology, (2009) 20(9), 095401. <https://doi.org/10.1088/0957-0233/20/9/095401>
- [7] M. Nassar, P. A. Vázquez, N. Chauris, M. Daaboul, A. Michel and C. Louste, "Experimental Models of the Variation of HFE-7100 and HFE-7000 Electric Properties With Temperature," IEEE Transactions on Industry Applications, vol. 56, no. 4, pp. 4193-4199, July-Aug. (2020).
- [8] P. Atten and J. Seyed-Yagoobi, " Electrohydrodynamically induced dielectric liquid flow through pure conduction in point/plane geometry", IEEE Trans. Dielec. Electr. Insul. 10 (2003) 23.
- [9] S.I. Jeong, J. Seyed-Yagoobi, P. Atten, "Theoretical/numerical study of electrohydrodynamic pumping through conduction phenomenon", IEEE Trans. Dielec. Electr. Insul. 39 (2003) 355.
- [10] Yazdani, M., & Seyed-Yagoobi, J., "Effect of charge mobility on dielectric liquid flow driven by EHD conduction phenomenon", Journal of Electrostatics, (2014), 72(4), 285-294. <https://doi.org/10.1016/j.elstat.2014.04..>